PROCEEDINGS, Sixteenth Workshop on Geothermal Reservoir Engineering
Stanford University, Stanford, California, January 23-25, 1991
SGP-TR-134

Two-Phase Flow Visualization and Relative Permeability Measurement in Transparent Replicas of Rough-Walled Rock Fractures

P. Persoff, K. Pruess, and L. Myer

Earth Sciences Division, Lawrence Berkeley Laboratory,
University of California, Berkeley, CA 94720

ABSTRACT

Understanding and quantifying multi-phase flow in fractures is important for mathematical and numerical simulation of geothermal reservoirs, nuclear waste repositories, and petroleum reservoirs. While the cubic law for single-phase flow has been well established for parallel-plate fractures theoretically and experimentally, no reliable measurements of multi-phase flow in fractures have been reported. This work reports the design and fabrication of an apparatus for visualization of two-phase flow and for measurement of gas-liquid relative permeability in realistic rough-walled rock fractures. A transparent replica of a natural rock fracture from a core specimen is fabricated by molding and casting in clear epoxy. Simultaneous flow of gas and liquid with control of capillary pressure at inlet and outlet is achieved with the Hassler "sandwich" design: liquid is injected to the fracture through a porous block, while gas is injected directly to the edge of the fracture through channels in the porous block. A similar arrangement maintains capillary separation of the two phases at the outlet. Pressure drops in each phase across the fracture, and capillary pressures at the inlet and outlet, are controlled by means of pumps and needle valves, and are measured by differential and absolute pressure transducers. The clear epoxy cast of the natural fracture preserves the geometry of the fracture and permits visual observation of phase distributions. The fracture aperture distribution can be estimated by filling the fracture with a dyed liquid, and making pointwise measurements of the intensity of transmitted light. A set of two-phase flow experiments has been performed which has proven the viability of the basic experimental design, while also suggesting further improvements in the apparatus. Preliminary measurements are presented for single-phase permeability to liquid, and for relative permeabilities in simultaneous flow of liquid and gas.

INTRODUCTION

Understanding and quantifying multi-phase flow in fractures is important for mathematical and numerical simulation of geothermal reservoirs, nuclear waste repositories, and petroleum reservoirs. When two (or more) phases occupy the pore space in a permeable material, pores occupied by one phase are unavailable for flow by the other; each phase interferes with the flow of the other. In porous media, this interference is quantified by relative permeability functions, defined by

$$k_i = k k_{rel,i} \qquad (1)$$

where k_i is the effective permeability to phase i, k is the intrinsic permeability of the medium, and $k_{rel,i}$ is the relative permeability to phase i. When the medium is completely saturated with phase i, $k_{rel,i} = 1$. The $k_{rel,i}$ are strong functions of phase saturation, and are therefore critical to the mathematical modeling of multiphase flow. Such functions should be equally important for modeling multiphase flow in fractures. While the cubic law for single-phase flow in parallel-plate fractures has been well established theoretically and experimentally (Witherspoon et al. 1980), no reliable measurements of multi-phase flow in fractures have been reported. Pruess and Tsang (1989, 1990) reviewed limited theoretical and experimental work, and presented a method by which relative permeability functions could be derived from fracture geometry. The laboratory investigation of Romm (1966) and analysis of field data for fractured geothermal reservoirs by Pruess et al. (1983, 1984) and by Bodvarsson et al. (1987) both suggested that

$$k_{rel,w} + k_{rel,nw} = 1 \qquad (2)$$

for all values of saturation, where w and nw denote the wetting and non-wetting phases, respectively. Constancy of the sum indicates negligible phase interference. However, results of numerical simulation using stochastically generated single-fracture geometries by Pruess and Tsang (1989, 1990) showed strong phase interference, with the sum much less than 1 at intermediate saturations. Romm (1966) used parallel-plate fractures (i.e., unrealistic fracture geometry); and in systems with phase changes, such as geothermal reservoirs, the phase interference is much less than in flow systems without phase changes; so $\sum_i k_{rel,i} = 1$ may not apply to fractures in general.

One of the goals of the present work is to resolve the apparent discrepancy between these results. This paper

reports the design and fabrication of an apparatus for visualizing two-phase flow and measuring gas-liquid relative permeability in realistic rough-walled rock fractures. We also present preliminary relative permeability data for gas-liquid flow in a transparent replica which reproduces the geometry of a natural fracture.

APPARATUS

The apparatus was designed to measure the inlet and outlet pressures of two immiscible fluids as they flow through a transparent epoxy resin cast of both sides of a natural rough-walled rock fracture (see Figure 1). Special endcaps were fabricated to inject and receive two immiscible fluids (gas, water, or oil) at controlled rates and pressures. The method of Hassler (1944) with porous endcaps was used to avoid capillary end effects and maintain uniform capillary pressure $p_{cap} \equiv p_{gas} - p_{liq}$ across the entire fracture plane. The multiphase fluids can be observed visually, and recorded with video equipment or still photography.

Transparent Fracture Replica

The centerpiece of the apparatus is a clear 7.6 cm × 7.6 cm epoxy resin cast of both sides of a natural rough-walled rock fracture. The fracture was approximately perpendicular to the axis of an 11.5-cm diameter granite core from the Stripa mine, Sweden. Rhodorsil RTV 1556 silicone rubber (Rhone-Poulenc, Inc., Monmouth Junction, NJ) was used to make molds of each side of the fracture (yielding a "negative" of the fracture-wall topography). Then Eccobond 27 clear epoxy (Emerson and Cuming, Dewey and Almy Chemical Division, W. R. Grace Co., Canton, MA) was used in the mold to make replicas (positive) of the surface of each side of the fracture. Both the silicone rubber and the epoxy are viscous two-part liquid formulations, and many air bubbles were entrained during mixing. Bubbles were eliminated by placing the container in a vacuum chamber and expanding the bubbles until they rose and burst. The liquid was then poured into the mold (or onto the original fracture surface) and evacuation was repeated. The silicone rubber was cured at room temperature, and the epoxy was cured at 100°C for 4 hr. The epoxy replicas were mated and machined to a 3-inch square section of the fracture; the outer surfaces were also machined and polished flat and parallel. Holes were drilled through a separate block of the cured epoxy for capillary rise measurements; these measurements showed that water wets the cured epoxy with zero contact angle.

Endcaps

Special endcaps were fabricated to inject and receive two immiscible fluids at controlled rates and pressures. For these experiments, distilled water and nitrogen gas were used as the wetting and non-wetting phases, respectively. The purpose of the endcaps is to maintain a difference between the pressures in the wetting and non-wetting phases at the upstream and downstream edges of the fracture. The design of Hassler (1944) for measuring relative permeability in porous cores was modified for fractures. Essentially, the wetting phase is delivered to the fracture edge through a wettable porous block, while the non-wetting phase is delivered through grooves in the porous block (Fig. 1). The grooves alternate with the flats between the grooves to cover the entire fracture edge in sections 0.05-inch long. The block was machined from porous ceramic with pore size controlled to have a 1-bar air-entry pressure (Soilmoisture Equipment Co., Santa Barbara, CA). Therefore, as long as the capillary pressure at inlet or outlet was less than one bar, the phases would remain separated, and no gas could back up into the water injection line. The porous block was cemented into a brass casing using quick-setting epoxy (Double Bubble, Hardman Co., Belleville, NJ). Liquid was delivered through four stainless steel tubes cemented into holes in the block, and gas was delivered through a single tube into a plenum which connected all the grooves.

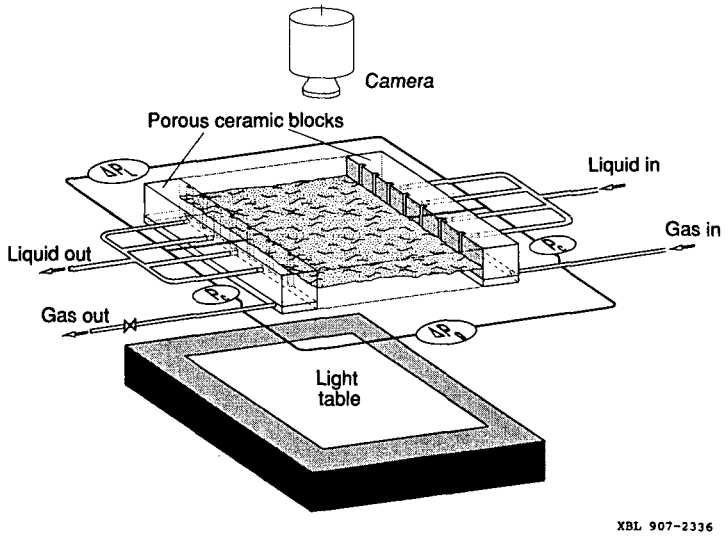

Figure 1. Apparatus for flow visualization and relative permeability measurement in transparent replica of a natural rock fracture. Ovals represent differential pressure transducers; absolute pressure transducers have been omitted for clarity. Note that gas is injected to a plenum which distributes it to vertical grooves in the porous block at the inlet end. Only seven grooves are shown in the figure; actually they are closely spaced with a total of 40 grooves. Rubber-lined steel bars which seal edges are not shown.

Control and Measurement of Flow Rates and Pressures

Four pressure taps sensed inlet and outlet gas pressure, and inlet and outlet liquid pressure. The gas pressure taps were located in the gas injection lines just outside the endcaps. In order to measure liquid pressure right at the fracture edges, a 0.25-inch hole was drilled completely through each porous block, and a liquid-pressure tap was cemented into this hole. The end of each liquid-pressure tap was filled with a plug of the same porous ceramic to prevent gas from invading the liquid-pressure tap (this is essentially the same as in Hassler's design). Absolute pressure transducers were used to measure the downstream absolute gas and liquid pressures, and differential pressure transducers were used to measure the inlet and outlet capillary pressures, and the pressure drops across the fracture in the gas and liquid phases (AP-10 and DP-15, Validyne Engineering Corp., Northridge, CA). This scheme permitted some redundancy and checking of measured pressures. Additionally, Bourdon-tube pressure-vacuum gauges were placed at all pressure taps and on the liquid lines bracketing the porous blocks. Micrometer needle valves (SS-2, Nupro Co., Willoughby, OH) were placed on both the gas and liquid outlet lines, to permit adjustment of each of the phase pressures at the outlet. During an experiment, inlet capillary pressure is set by flow rates; outlet capillary pressure is adjusted with the needle valves to equal it. Pressures and gas flow rates were automatically recorded.

The liquid flow was delivered by an LC-5000 syringe pump (ISCO, Lincoln, NE). Because the pump capacity is limited to 500 mL, it was occasionally necessary to refill the pump during the experiment, which takes about 5 minutes. To continue uninterrupted liquid flow during this time, a liquid reservoir was connected to the liquid injection line, and pressurized with nitrogen to the pressure indicated by the appropriate gauge. This allowed liquid delivery to continue at the same pressure that had existed during constant-rate delivery.

Gas was delivered through either of a pair of Brooks 5850E mass-flow controllers (Emerson Electric, Hatfield, PA), with capacities of 10 and 1000 mL/min at standard temperature and pressure.

Before assembling the endcaps to the inlet and outlet edges of the transparent fracture replica, a piece of glass-fiber filter (Reeve Angel 934 AH, Whatman, Inc., Clifton, NJ) was placed over the grooved face of the porous block to ensure liquid-phase capillary continuity. The filter was wetted and a scalpel was used to make slits in it over the grooves. Thus both gas and liquid had access to the fracture edges. The endcaps were placed over the fracture edges, and pressed against the fracture edges by means of threaded tension rods.

To confine all fluid flow to the fracture, the no-flow edges and the circumferences of the end caps were sealed. This was accomplished by six steel bars lined with 1/16" thick silicone rubber, which were pressed against the fracture replica by threaded rods. The fracture itself was loaded in compression between a pair of machined lucite blocks, using four Belleville spring washers (Associated Spring Gardena, CA) to apply a total load of 240 lb. over the 9 square inch area, corresponding to 26.7 psi. The entire assembly was leak tested under water at 20 psi gas pressure.

EXPERIMENTAL PROCEDURE

The apparatus was evacuated to a pressure above the vapor pressure of water, and water was injected to saturate the fracture and the porous blocks. Liquid permeability measurements were made at a range of flow rates. During this phase of the experiment, the portions of the apparatus that were designed to be gas-filled in two-phase flow conditions were liquid-filled (the liquid was later displaced when gas was admitted to the apparatus). This allowed two measurements each of the liquid inlet and outlet pressure, using the pressure taps normally dedicated to gas and liquid. These pairs of measurements did not agree at the outlet, the pressure measured by the liquid pressure tap was approximately 0.2 psi higher than that measured by the gas pressure tap, while at the inlet the pressure measured by the gas pressure tap was approximately 0.1 psi higher than that measured by the liquid pressure tap. These discrepancies result from the heterogeneity of the fracture. The gas pressure tap is connected to many distributed grooves, and thus averages over the entire edge (inlet or outlet) of the fracture, while the liquid pressure tap senses liquid only at one point along the edge. For non-uniform apertures, the pressure will generally not be uniform along the edge, especially at the outlet edge.

Several hours were needed for the liquid pressure transducers to attain steady readings in response to changes in the flow rate. This slow response resulted from the relatively low permeability of the porous endcaps (approximately 8 millidarcy) and from the presence of air bubbles which could not be eliminated from pressure taps and transducers. For a change in water pressure in the fracture to be felt by the transducer, enough water must flow through the porous plugs in the liquid pressure taps to compress the bubbles. To test for liquid leaks, the apparatus was pressurized and shut in. The pressures recorded during 24 hours showed that there was no leakage of liquid, but pressure variation during the day suggested that pressures changed with diurnal (day/night) variation in ambient temperatures.

After measuring the liquid permeability, two-phase flow was initiated by starting gas injection to the fracture. Gas displaced liquid from the endcap grooves and plenums, and made a flow path from inlet to exit. Visual observations were made, and pressure measurements were continued to steady state, and then the gas flow rate was increased and the liquid flow rate decreased stepwise to reach a new steady state. For each steady state after the first, the needle valve on the gas outlet line was

adjusted to get the outlet and inlet capillary pressure approximately equal, and each steady state was maintained for 24 hr or longer before proceeding to the next. Measurements were made at a series of eight flow conditions with gas-to-liquid flow rate ratios varying over three orders of magnitude.

Permeability Calculation

The permeability of a porous medium to gas is calculated by (Scheidegger, 1974)

$$k_g = \frac{2q_o\mu L p_o}{(p_i^2 - p_o^2)} \tag{3}$$

where k is permeability, q is the darcy flow velocity or volumetric flux [L/t], μ is the viscosity, L is the length from inlet to outlet, subscripts i and o represent inlet and outlet conditions, respectively, and subscript g refers to gas. If flow is not through a porous medium but through a series of parallel fractures with spacing h, then both sides of equation (3) can be multiplied by h to give

$$hk_g = \frac{2hq_o\mu L p_o}{(p_i^2 - p_o^2)} \tag{4}$$

Without knowledge of the fracture aperture, the value of q_o is not known, but the value of hq_o is known from continuity:

$$hq_o = \frac{Q_o}{w} \tag{5}$$

where Q is the volumetric flow rate [L^3/t] and w is the length of the fracture edge at inlet and outlet. Similarly, k_{liq} can not be measured, but hk_{liq} can be:

$$hk_{liq} = \frac{hq\mu L}{p_i - p_o} \tag{6}$$

where $hq = Q/w$; for incompressible fluids Q and q do not vary from inlet to outlet.

Relative permeabilities were calculated by normalizing the measured effective gas and liquid permeabilities to the liquid permeability of the fracture. To calculate ratios of gas and liquid flow rates, the gas flow rate was evaluated at the arithmetic average of the inlet and outlet gas pressures.

RESULTS

Competition between Gas and Liquid For Pore Occupancy

We view a rough-walled fracture as a two-dimensional heterogeneous porous medium, with pore sizes (apertures) varying across the fracture plane (Pruess and Tsang, 1989, 1990). Capillary theory then suggests that in gas-liquid flow in a fracture, the larger pore spaces will be occupied by gas, and the smaller ones by liquid. As long as the pressures and flow rates do not change, the pore occupancy should be static. Our visual observations of the fracture during two-phase flow conditions, however, indicated that there may not be a true steady state on the pore scale. We frequently observed events in which pores switched between gas and liquid occupancy, especially in liquid-dominated conditions. In a typical liquid-dominated flow condition, part of the gas flow path was always occupied by gas, but several stretches of the gas flow path were intermittently occupied by liquid. Trains of bubbles could be seen, separated by liquid, migrating through these stretches. Typically, no action (that is, no changes of pore occupancy) would be seen for a few minutes, then a train of bubbles would be seen to move through part of the gas flow path. A few seconds later, a train of bubbles would be seen marching through a second stretch of the gas flow path, and so on. These were portions of the flow path which were sometimes occupied by liquid. Two-phase flow shows structure on a small scale; many gas flow paths appear tube-like with width of order 1 mm or less in the fracture plane. To reconcile this picture of flow with the local-parallel-plate model of Pruess and Tsang (1989, 1990) might require an impracticably fine space discretization.

Additionally, in liquid-dominated flow regimes, steady pressures could not be reached; rather the system was disturbed by regular "hiccups" as shown in Figures 2a and 2b. Visual observations during these events showed that they were caused by periodic invasion and blockage of the gas flow path by liquid. A temporary blockage of the gas flow path caused the upstream gas pressure to increase, and the downstream gas pressure to decrease, as shown in Figure 2b. Visual observation while this happened showed that all gas flowed through a critical path (choke point) near one side edge of the fracture. A dead-end gas-filled pore upstream of the choke point became larger, acting as a surge chamber, until the pressure drop across the blocked throat became great enough for gas to displace water from the throat, and flow was restored, with several bubble trains flowing toward the exit as described earlier. The repeated reinvasion of gas filled pores by liquid is similar to the "snap-off" events described by Ransohoff and Radke (1988), except that the liquid films between buboles in our experiment collapsed instantly because they were not stabilized by surfactant. At dryer conditions, less water was available to invade gas flow paths and the throat-clearing events become less frequent and eventually cease altogether. Typical inlet and outlet pressures measured during a dryer steady state are shown in Figure 3, while typical inlet and outlet capillary pressures are shown in Figure 4.

Relative Permeability Data

Table 1 summarizes the steady-state data measured during single-phase flow of liquid and eight two-phase flow conditions, measured in order of increasing dryness. Note that equality of inlet and outlet capillary pressures was only achieved approximately. The values shown represent average values during a 24-hour or longer period.

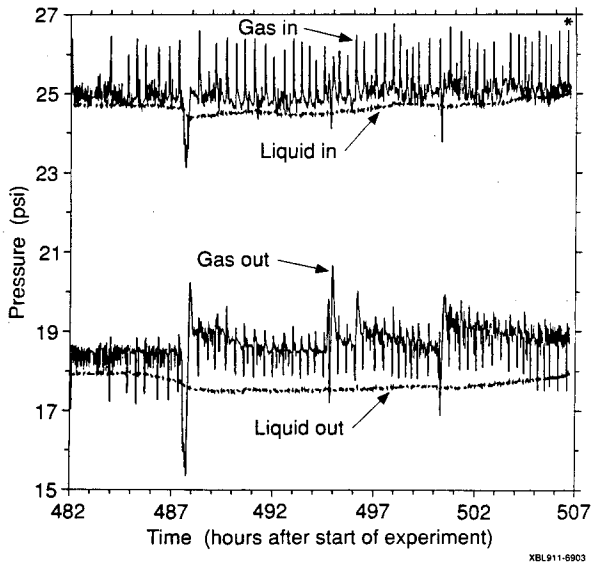

Figure 2a. Inlet and outlet fluid pressures measured during "steady" state with q_{gas}/q_{liq} = 9.5. The inlet and outlet capillary pressures were not equalized at this steady state. Note regular "hiccups" which result from blocking and clearing of gas flow path.

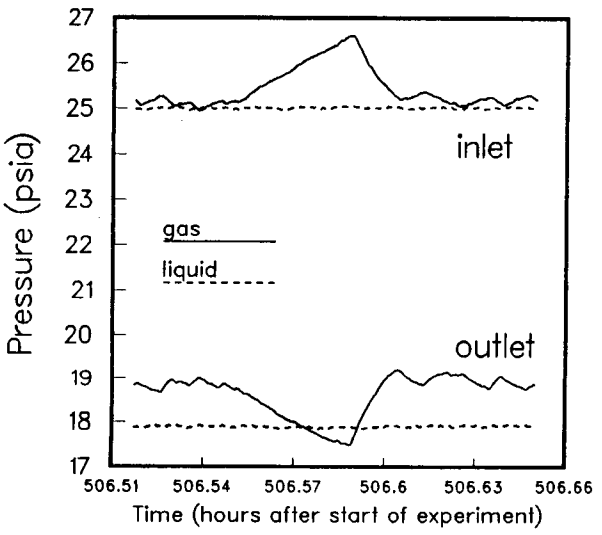

Figure 2b. Event marked by * in Figure 2a.

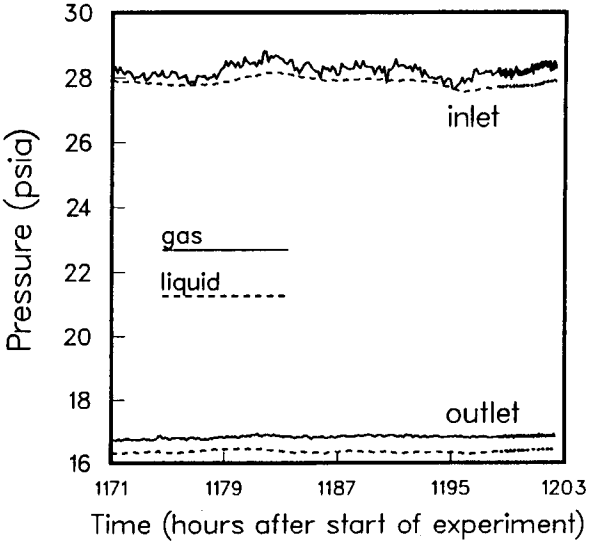

Figure 3. Inlet and outlet fluid pressures measured during steady state with q_{gas}/q_{liq} = 900. This is a dryer condition than shown in Figure 2, and "hiccups" did not occur.

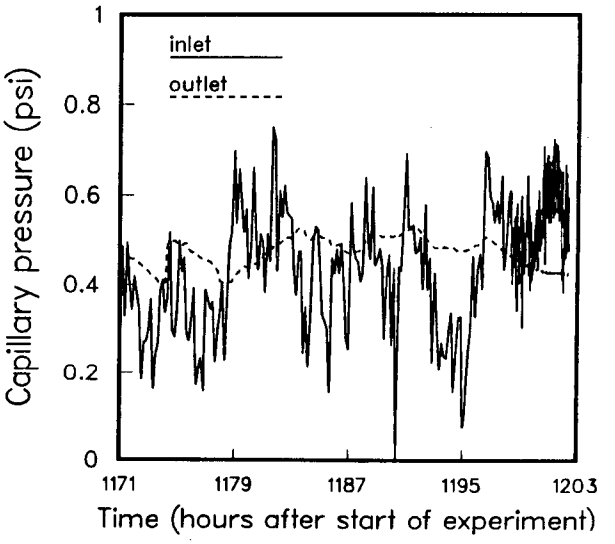

Figure 4. Inlet and outlet capillary pressures measured during steady state with q_{gas}/q_{liq} = 900.

The results for relative permeabilities are plotted in Figures 5 and 6. In Figure 5 the data were plotted against the gas:liquid flow rate ratio rather than against volumetric saturation, because volumetric phase saturations were not measured. In Figure 6, the gas and liquid relative permeabilities are plotted against each other to indicate the degree of phase interference. In both Figures 5 and 6, typical relative permeability curves for porous media are plotted for comparison. These curves were calculated using the formulas given by Corey (1954):

$$k_{rel,liq} = (S^*)^4 \quad (7)$$

$$k_{rel,gas} = (1-(S^*)^2)(1-S^*)^2 \quad (8)$$

where S is saturation, $S^* = (S_{liq}-S_{liq,r})/(1-S_{liq,r}-S_{gas,r})$, and subscript r refers to residual saturation. The Corey curves were calculated with the commonly used values of $S_{gas,r} = 0.05$ and $S_{liq,r} = 0.30$.

Table 1. Flow rates, pressures, and permeabilities

Flow rates		Pressures			Capillary pressures		Permeabilities			
$hq_{o,g}$ (m^2/s)	hq_{liq} (m^2/s)	$p_{g,i}$ (kPa)	$p_{g,o}$ (kPa)	Δp_{liq} (kPa)	inlet (kPa)	outlet (kPa)	hk_g (m^3)	hk_{liq} (m^3)	$k_{rel,g}$	$k_{rel,liq}$
liquid flow								5.09E-17		1.00
7.65E-8	8.02E-9	173.7	130.3	47.4	2.34	8.96	2.01E-18	1.29E-17	0.0395	0.2530
1.61E-7	8.02E-9	179.3	126.9	52.9	2.55	2.55	3.39E-18	1.16E-17	0.0666	0.2271
3.15E-7	8.02E-9	180.6	127.6	56.7	2.97	1.86	6.58E-18	1.08E-17	0.1292	0.2118
5.60E-7	8.02E-9	187.5	127.9	59.3	2.76	2.62	1.01E-17	1.03E-17	0.1994	0.2026
1.04E-6	8.02E-9	199.9	128.2	70.7	3.03	1.03	1.52E-17	8.65E-18	0.2970	0.1699
3.30E-6	2.73E-9	194.8	115.5	79.4	3.03	3.24	4.13E-17	2.62E-18	0.8132	0.0515
4.37E-6	1.37E-9	188.9	112.0	80.0	3.59	3.59	5.65E-17	1.31E-18	1.1092	0.0256
5.75E-6	5.47E-10	180.6	107.2	73.2	3.65	3.38	7.77E-17	5.69E-19	1.5273	0.0112

DISCUSSION

Fracture Aperture

The effective average aperture of the fracture can be estimated from the data using the cubic law: the permeability of a parallel plate aperture of thickness b is $b^2/12$. If a series of such apertures are separated by distance h, then the average permeability of the fractured medium is $(b^2/12)(b/h)$. Then

$$b = \sqrt[3]{12kh} \tag{9}$$

Using the experimentally determined value for hk_{liq} (Eq. 6), this gives an "average" aperture for the fracture of 8.5 μm. But because permeability is controlled by the smallest apertures, it is likely that the volume of the fracture divided by its area is much larger.

The aperture at critical pore throats can also be estimated. The visual observations of "throat-clearing" events such as shown in Figure 2b suggest that gas flow is blocked at a single pore throat. Assuming that the pressure drop across that throat increases until essentially all the pressure drop across the fracture occurs at that throat, the Young-Laplace law can be used to estimate the radius of the critical throat from the interfacial tension and observed pressure drop:

$$r = \frac{2\sigma}{\Delta p} \tag{10}$$

Reading the pressures from Figure 2b as 26.6 and 17.5 psi, (Δp = 9.1 psi = 62.7 kPa) and taking the surface tension σ as 0.07 N/m, then the radius is 2.2 μm, which agrees qualitatively with the estimate of "average" aperture.

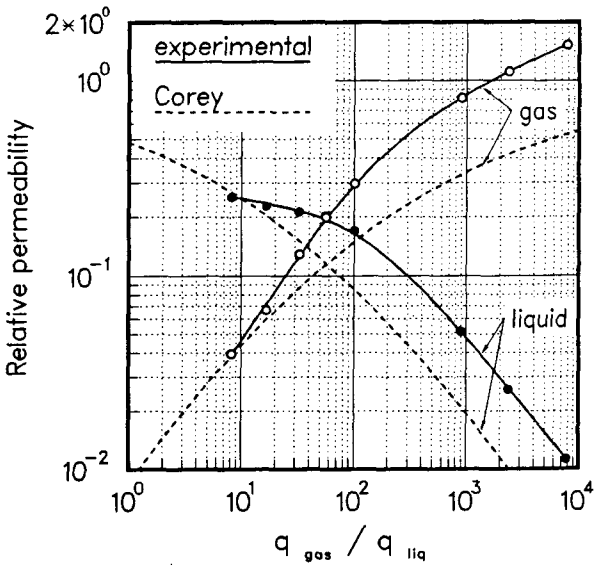

Figure 5. Relative permeabilities during steady states, plotted against ratio of flow rates. For comparison, a curve typical of porous media (Corey, 1954) is also plotted.

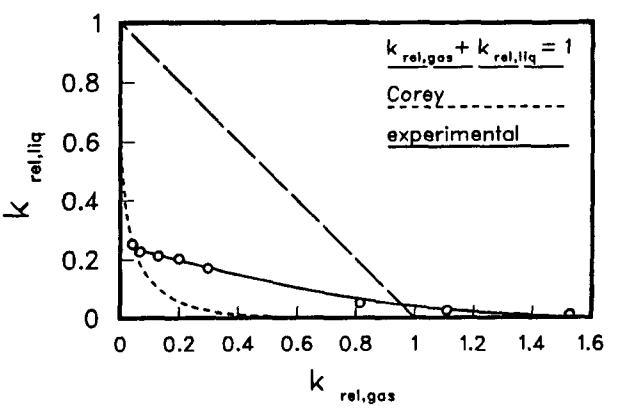

Figure 6. Gas and liquid relative permeabilities plotted against each other. For comparison, $k_{rel,gas} + k_{rel,liq} = 1$ and a curve typical of porous media (Corey 1954) are also plotted.

Control of Capillary Pressures

One of the intended goals of this work is that the outlet capillary pressure be controlled to equal the inlet capillary pressure. Because of the noisiness in the measured capillary pressures shown in Figure 4, this goal has only been achieved approximately. However, the inlet capillary pressures shown in Table 1 display reasonable behavior with changes in liquid saturation and flow rate ratio.

Figures 2a and 3, as well as the data collected at other steady states, show that the outlet pressures are relatively steady but the inlet pressures are more noisy. Because the outlet pressures are directly measured, but the inlet pressures are calculated as the sum of two measurements, the extra noise in the inlet pressure may be an artifact, resulting from accumulated experimental error. But such noise may also reflect many changes of phase occupancy, too small to cause the events shown in Figures 2a and 2b. In single-phase liquid flow, the calculated inlet pressures were no noisier than the outlet pressures. This suggests that the additional noise in the inlet pressures in two-phase flow is real. Additional absolute pressure taps will be added at the inlet end to confirm this.

The noise in capillary pressure measurements may also be an artifact, caused by differences in response time between the gas and liquid pressure taps. The gas pressure taps respond much more rapidly than the liquid pressure taps. It is therefore possible that the actual capillary pressure is steady while gas and liquid pressure vary together, but the measured capillary pressure reflects the lag in the liquid pressure taps.

During two-phase flow, the ratio of volumetric flow rates was varied from all liquid with no gas flowing, to a ratio of gas/liquid = 8000. Visual observations showed increasing gas saturation during the steady states, with the edges of the fracture desaturating first, and the center last. This means that the center of the fracture is the region of contact, with widest apertures and preferential flow paths for non-wetting fluid around the outside. Fracture apertures have not been measured but are expected to confirm this. This configuration suggests that some slight warpage of either the epoxy casts or silicone rubber molds may have occurred during curing. As such, it represents a deviation from the realistic fracture geometry which was intended. However, the roughness of the surfaces still appears to be accurately represented, and the localized contact area with regions of greater aperture is still typical of natural fractures.

Table 1 shows that gas relative permeability increases beyond 1, which may be due to experimental error or to non-Darcy flow effects. The cause of this discrepancy will be elucidated in further experiments.

IMPROVEMENTS TO THE APPARATUS

The preliminary results presented here confirm the feasibility of using the Hassler "sandwich" design for measuring relative permeability in fractures, and of observing phase saturation distribution in transparent fractures. However, they also indicate the need for several improvements which will be made for further experiments:

The molding technique will be improved so that the two sides of the fracture replica mate as well as the original rock. The tendency of the fracture replica to have a contact region only in the center can also be compensated for in the design of the compressing lucite blocks.

The number of liquid pressure taps in each end will be increased, so that liquid pressure will represent an average over the edge rather than a point value. The thickness of the porous blocks in the liquid pressure taps will be reduced, and gas bubbles in the liquid pressure taps eliminated, to reduce the response time of the liquid pressure measurements. Additional absolute pressure transducers will also be placed at the inlet.

The temperature will be controlled to eliminate day/night changes in pressure gradients that have been observed.

The fracture will be filled with a dyed liquid so that the fracture aperture can be estimated at every point using the measured intensity of transmitted light (see Cox et al., 1990).

A video camera with digital image processing capabilities will be added to allow analysis of saturation data.

Experiments will be done with actual rock fractures. This will lose the visualization capability, but gain realism in the fracture geometry and the wettability of surfaces.

SUMMARY AND PRELIMINARY CONCLUSIONS

Flow visualization has provided evidence that even for very slow flows, there may be no true steady states. Instead there is a continual succession of transient changes in phase occupancy at critical pore throats. At large values of liquid saturation, sufficient liquid is available to intermittently block some of the gas flow paths (or, in extreme cases, the only gas flow path). This results in continual episodes of throat blocking and clearing, as shown in Figure 2b. Such behavior is not generally observed in porous media, perhaps due to the much larger number of flow paths in typical sample sizes.

The limited experiments carried out so far have confirmed the viability of the Hassler design for achieving two-phase flow conditions in a small fracture under

well-defined capillary conditions, without end effects. A series of quasi-steady two-phase flow conditions has been achieved. Quantitative analysis is hampered by diurnal pressure fluctuations caused by temperature fluctuations in the laboratory. However, some preliminary conclusions can be drawn. The relative permeability data plotted in Figures 5 and 6 show that strong phase interference occurs between the gas and liquid phases, with the sum of gas and liquid relative permeabilities much less than 1 at intermediate saturations. The shapes of the curves suggest that phase interference occurs in fractures in much the same manner as in porous media.

ACKNOWLEDGMENTS

The authors are indebted to Marcelo Lippmann for a critical review of the manuscript. This work was supported by the Assistant Secretary for Conservation and Renewable Energy, Office of Renewable Energy Technologies, Geothermal Technology Division of the U.S. Department of Energy, under Contract no. DE-AC03-76SF00098. The use of brand names in this paper is for identification purposes only and does not imply endorsement by LBL or DOE.

REFERENCES

Bodvarsson, G. S., Pruess, K., Stefansson, V., and Ojiambo, S. B. (1987). East Olkaria geothermal field, Kenya, 1, History match with production and pressure decline data. *J. Geophys. Res. 92,* (B1), 521-539.

Corey, A. T. (1954). The interrelationship between gas and oil relative permeabilities, *Prod. Mon. 19,* 38-41.

Cox, B. L., Persoff, P., and Pruess, K. (1990). A casting and imaging technique for determining void geometry and relative permeability behavior of a single fracture specimen. paper presented at the Fifteenth Workshop on Geothermal Reservoir Engineering, Stanford Univ., Stanford, CA.

Hassler, G. L. (1944). Method and Apparatus for Permeability Measurements, U.S. Patent 2,345,935. April 4.

Pruess, K.. Bodvarsson, G. S., and Stefansson, V. (1983). Analysis of production data from the Krafla geothermal field, Iceland, Proc. Ninth Workshop on Geothermal Reservoir Engineering, Stanford Univ., Stanford, CA, pp. 345-350.

Pruess, K., Bodvarsson, G. S., Stefansson, V., and Eliasson, E. T. (1984). The Krafla geothermal field, Iceland, 4, History match and prediction of individual well performance, *Water Resources Research, 20* (11), 1561-1584.

Pruess, K. and Tsang, Y. W. (1989). On relative permeability of rough-walled fractures, Proc. Fourteenth Workshop on Geothermal Reservoir Engineering, Stanford Univ., Stanford, CA. pp. 123-130.

Pruess, K. and Tsang, Y. W. (1990). On two-phase relative permeability and capillary pressure in rough-walled rock fractures, *Water Resources Research, 26* (9), 1915-1926.

Romm, E. S. (1966). *Fluid Flow in Fractured Rocks* (in Russian), Nedra Publishing House, Moscow. (English translation, W. R. Blake, Bartlesville, OK, 1972.)

Ransohoff, T. C. and Radke, C. J. (1988). Mechanisms of foam generation in glass-bead packs, *SPE Reservoir Engineering,* May, 573-585.

Scheidegger, A. E. (1974). *The Physics of Flow Through Porous Media,* 3rd ed., University of Toronto Press, Toronto, p. 102.

Witherspoon, P. A., Wang, J. S. W., Iwai, K., and Gale, J. E. (1980). Validity of Cubic Law for Fluid Flow in a Deformable Rock Fracture, *Water Resources Research, 16,* (6) 1016-1024.